



# Calibration of an Astrophysical Spectrograph Below 1 m/s Using a Laser Frequency Comb

## Citation

Phillips, David F., Alexander G. Glenday, Chih-Hao Li, Claire Cramer, Gabor Furesz, Guoqing Chang, Andrew J. Benedick, et al. 2012. Calibration of an Astrophysical Spectrograph Below 1 m/s Using a Laser Frequency Comb. *Optics Express* 20, no. 13: 13711-13726.

## Published version

<https://doi.org/10.1364/OE.20.013711>

## Link

<http://nrs.harvard.edu/urn-3:HUL.InstRepos:11878774>

## Terms of use

This article was downloaded from Harvard University's DASH repository, and is made available under the terms and conditions applicable to Other Posted Material (LAA), as set forth at

<https://harvardwiki.atlassian.net/wiki/external/NGY5NDE4ZjgzNTc5NDQzMGIzZWZhMGFIOWI2M2EwYTg>

## Accessibility

<https://accessibility.huit.harvard.edu/digital-accessibility-policy>

## Share Your Story

The Harvard community has made this article openly available. Please share how this access benefits you. [Submit a story](#)

# Calibration of an astrophysical spectrograph below 1 m/s using a laser frequency comb

David F. Phillips,<sup>1,\*</sup> Alexander G. Glenday,<sup>1</sup> Chih-Hao Li,<sup>1</sup> Claire Cramer,<sup>1,6</sup> Gabor Furesz,<sup>1,2</sup> Guoqing Chang,<sup>3</sup> Andrew J. Benedick,<sup>3,7</sup> Li-Jin Chen,<sup>3,8</sup> Franz X. Kärtner,<sup>3,4</sup> Sylvain Korzennik,<sup>1</sup> Dimitar Sasselov,<sup>1</sup> Andrew Szentgyorgyi,<sup>1</sup> and Ronald L. Walsworth<sup>1,5</sup>

<sup>1</sup> *Harvard-Smithsonian Center for Astrophysics, 60 Garden St., Cambridge MA 02138, USA*

<sup>2</sup> *Konkoly Observatory of the Hungarian Academy of Sciences, Budapest, Hungary*

<sup>3</sup> *Department of Electrical Engineering and Computer Science and Research Laboratory of Electronics, Massachusetts Institute of Technology, 77 Mass. Ave Cambridge MA 02139, USA*

<sup>4</sup> *Physics Dept., Hamburg University and DESY, Hamburg, Germany*

<sup>5</sup> *Dept. of Physics, Harvard University, Cambridge MA, 02138, USA*

<sup>6</sup> *Now at National Institutes of Standards and Technologies, 100 Bureau Drive, Gaithersburg, MD, 20899, USA*

<sup>7</sup> *Now at MIT Lincoln Laboratory, 244 Wood Street, Lexington, MA 02421, USA*

<sup>8</sup> *Now at IdestaQE, 435 Route 206 N, Newton, NJ 07860, USA*

[\\*dphil@cfa.harvard.edu](mailto:dphil@cfa.harvard.edu)

**Abstract:** We deployed two wavelength calibrators based on laser frequency combs (“astro-combs”) at an astronomical telescope. One astro-comb operated over a 100 nm band in the deep red ( $\sim 800$  nm) and a second operated over a 20 nm band in the blue ( $\sim 400$  nm). We used these red and blue astro-combs to calibrate a high-resolution astrophysical spectrograph integrated with a 1.5 m telescope, and demonstrated calibration precision and stability sufficient to enable detection of changes in stellar radial velocity  $< 1$  m/s.

© 2012 Optical Society of America

**OCIS codes:** (120.6200) Spectrometers and spectroscopic instrumentation; (300.0300) Spectroscopy.

---

## References and links

1. F. Pepe, C. Lovis, D. Ségransan, W. Benz, F. Bouchy, X. Dumusque, M. Mayor, D. Queloz, N. C. Santos, and S. Udry, “The HARPS search for Earth-like planets in the habitable zone,” *Astron. Astrophys.* **534**, A58, 1–16 (2011).
2. C. Lovis, M. Mayor, F. Pepe, Y. Alibert, W. Benz, F. Bouchy, A. C. M. Correia, J. Laskar, C. Mordasini, D. Queloz, N. C. Santos, S. Udry, J. Bertaux, and J. Sivan, “An extrasolar planetary system with three Neptune-mass planets,” *Nature* **441**, 305–309 (2006).
3. S. Udry, X. Bonfils, X. Delfosse, T. Forveille, M. Mayor, C. Perrier, F. Bouchy, C. Lovis, F. Pepe, D. Queloz, and J.-L. Bertaux, “The harps search for southern extra-solar planets,” *Astron. Astrophys.* **469**, L43–L47 (2007).
4. C. Li, A. J. Benedick, P. Fendel, A. G. Glenday, F. X. Kärtner, D. F. Phillips, D. Sasselov, A. Szentgyorgyi, and R. L. Walsworth, “A laser frequency comb that enables radial velocity measurements with a precision of  $1 \text{ cm s}^{-1}$ ,” *Nature* **452**, 610–612 (2008).
5. A. J. Benedick, G. Chang, J. R. Birge, L.-J. Chen, A. G. Glenday, C.-H. Li, D. F. Phillips, A. Szentgyorgyi, S. Korzennik, G. Furesz, R. L. Walsworth, and F. X. Kärtner, “Visible wavelength astro-comb,” *Opt. Express* **18**, 19175–19184 (2010).
6. M. T. Murphy, T. Udem, R. Holzwarth, A. Sismann, L. Pasquini, C. Araujo-Hauck, H. Dekker, S. D’Odorico, M. Fischer, T. W. Hänsch, and A. Manescau, “High-precision wavelength calibration of astronomical spectrographs with laser frequency combs,” *Mon. Not. R. Astron. Soc.* **380**, 839–847 (2007).

7. S. Osterman, S. Diddams, M. Beasley, C. Froning, L. Hollberg, P. MacQueen, V. Mbele, and A. Weiner, "A proposed laser frequency comb-based wavelength reference for high-resolution spectroscopy," in "Techniques and Instrumentation for Detection of Exoplanets III," Proc. SPIE, 66931G, 1–9 (2007).
8. T. Steinmetz, T. Wilken, C. Araujo-Hauck, R. Holzwarth, T. W. Hänsch, L. Pasquini, A. Manescau, S. D'Odorico, M. T. Murphy, T. Kentischer, W. Schmidt, and T. Udem, "Laser frequency combs for astronomical observations," *Science* **321**, 1335–1337 (2008).
9. D. A. Braje, M. S. Kirchner, S. Osterman, T. Fortier, and S. A. Diddams, "Astronomical spectrograph calibration with broad-spectrum frequency combs," *Euro. Phys. J. D* **48**, 57–66 (2008).
10. T. Wilken, C. Lovis, A. Manescau, T. Steinmetz, L. Pasquini, G. Lo Curto, T. W. Hänsch, R. Holzwarth, and T. Udem, "High-precision calibration of spectrographs," *Mon. Not. R. Astron. Soc. Lett.* **405**, L16–L20 (2010).
11. S. L. Redman, G. G. Ycas, R. Terrien, S. Mahadevan, L. W. Ramsey, C. F. Bender, S. N. Osterman, S. A. Diddams, F. Quinlan, J. E. Lawler, and G. Nave, "A high-resolution atlas of uranium-neon in the h band," *The Astrophys. J. Suppl. Ser.* **199**(2), 1–11 (2012).
12. G. G. Ycas, F. Quinlan, S. A. Diddams, S. Osterman, S. Mahadevan, S. Redman, R. Terrien, L. Ramsey, C. F. Bender, B. Botzer, and S. Sigurdsson, "Demonstration of on-sky calibration of astronomical spectra using a 25 GHz near-ir laser frequency comb," *Opt. Express* **20**, 6631–6643 (2012).
13. S. T. Cundiff and J. Ye, "Colloquium: Femtosecond optical frequency combs," *Rev. Mod. Phys.* **75**, 325–342 (2003).
14. T. Steinmetz, T. Wilken, C. Araujo-Hauck, R. Holzwarth, T. Hänsch, and T. Udem, "Fabry–Pérot filter cavities for wide-spaced frequency combs with large spectral bandwidth," *Appl. Phys. B* **96**, 251–256 (2009).
15. M. S. Kirchner, D. A. Braje, T. M. Fortier, A. M. Weiner, L. Hollberg, and S. A. Diddams, "Generation of 20 GHz, sub-40 fs pulses at 960 nm via repetition-rate multiplication," *Opt. Lett.* **34**, 872–874 (2009).
16. A. Benedick, J. Birge, R. Ell, O. D. Mucke, M. Sander, and F. X. Kärtner, "Octave spanning 1 GHz Ti:sapphire oscillator for HeNe CH<sub>4</sub>-based frequency combs and clocks," in *Lasers and Electro-Optics, 2007 and the International Quantum Electronics Conference, (CLEOE-IQEC 2007)*.
17. R. W. P. Drever, J. L. Hall, F. V. Kowalski, J. Hough, G. M. Ford, A. J. Munley, and H. Ward, "Laser phase and frequency stabilization using an optical resonator," *Appl. Phys. B* **31**, 97–105 (1983).
18. G. Furesz, "Design and application of high resolution and multiobject spectrographs: Dynamical studies of open clusters," Ph. D. thesis, University of Szeged, Hungary (2008).
19. J. Baudrand and G. A. H. Walker, "Modal noise in high-resolution, fibered spectra: A study and simple cure," *Publ. Astron. Soc. Pac.* **113**, 851–858 (2001).
20. N. E. Piskunov and J. A. Valenti, "New algorithms for reducing cross-dispersed echelle spectra," *Astron. Astrophys.* **385**, 1095–1106 (2002).
21. J. W. Brault, "High precision Fourier transform spectrometry: The critical role of phase corrections," *Microchimica Acta* **93**, 215–227 (1987).
22. C.-H. Li, A. G. Glenday, A. J. Benedick, G. Chang, L.-J. Chen, C. Cramer, P. Fendel, G. Furesz, F. X. Kärtner, S. Korzennik, D. F. Phillips, D. Sasselov, A. Szentgyorgyi, and R. L. Walsworth, "In-situ determination of astro-comb calibrator lines to better than 10 cm s<sup>-1</sup>," *Opt. Express* **18**, 13239–13249 (2010).
23. C. Lovis and F. Pepe, "A new list of thorium and argon spectral lines in the visible," *Astron. Astrophys.* **468**, 1115–1121 (2007).
24. T. R. Hunter and L. W. Ramsey, "Scrambling properties of optical fibers and the performance of a double scrambler," *Proc. Astro. Soc. Pac.* **104**, 1244–1251 (1992).
25. G. Chang, C.-H. Li, D. F. Phillips, R. L. Walsworth, and F. X. Kärtner, "Toward a broadband astro-comb: effects of nonlinear spectral broadening in optical fibers," *Opt. Express* **18**, 12736–12747 (2010).
26. L.-J. Chen, G. Chang, C.-H. Li, A. J. Benedick, D. F. Phillips, R. L. Walsworth, and F. X. Kärtner, "Broadband dispersion-free optical cavities based on zero group delay dispersion mirror sets," *Opt. Express* **18**, 23204–23211 (2010).
27. C.-H. Li, G. Chang, A. G. Glenday, D. F. Phillips, F. Kärtner, A. Szentgyorgyi, and R. L. Walsworth, "Conjugate Fabry-Perot cavity pair for astro-combs," submitted to *Opt. Lett.* (2012).
28. A. Sandage, "The change of redshift and apparent luminosity of galaxies due to the deceleration of selected expanding universes," *Astrophys. J.* **136**, 319–333 (1962).
29. A. Loeb, "Direct measurement of cosmological parameters from the cosmic deceleration of extragalactic objects," *Astrophys. J. Lett.* **499**, L111–L114 (1998).

---

## 1. Introduction

Over the past two decades, the discovery and characterization of exoplanets has progressed dramatically. In particular, precision radial velocity (PRV) measurements are now widely used to determine oscillatory stellar motion about the barycenter of an exo-solar system, providing a lower limit on exoplanet mass. This information is encoded in the periodic Doppler shift of

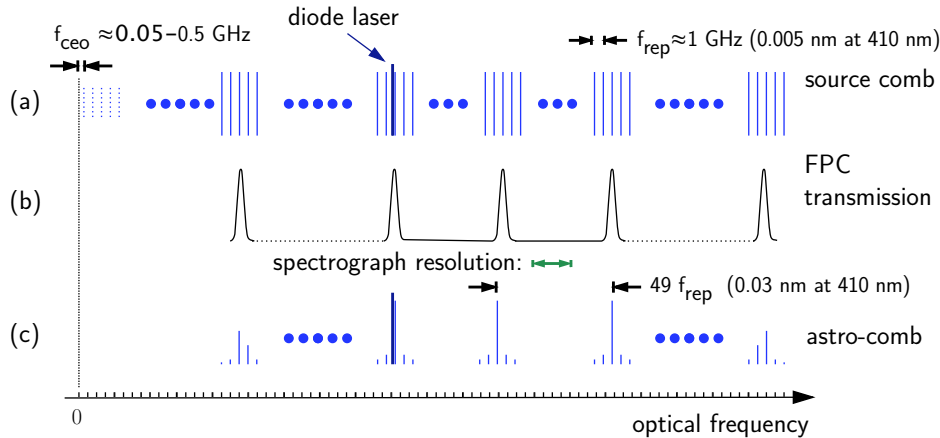


Fig. 1. Schematic representation of astro-comb spectrum. (a) Source comb spectrum with line spacing of 1 GHz ( $\approx 0.002 \text{ nm}$  at 800 nm) and a diode laser spectral line which provides a fiducial reference to determine the absolute frequency of the comb spectrum. (b) Fabry-Pérot Cavity (FPC) transmission spectrum spaced by 50 GHz. (c) Resultant astro-comb spectrum showing exaggerated unsuppressed comb lines (referred to as “side modes” in the text). Large dots represent source-comb lines left unshown for clarity.

stellar spectral features measured with high resolution astrophysical spectrographs. The current precision of such measurements has reached the 1 m/s level [1]. However, detection of exo-Earths, Earth-mass planets in the habitable zone around Sun-like stars, will require an order-of-magnitude improvement in PRV measurement sensitivity to below 10 cm/s. One of the key limitations of PRV measurements is precise and stable wavelength calibration of the astrophysical spectrograph [2, 3].

A crucial technology for these investigations is an ultrastable, broadband, high line-density, bright wavelength calibrator that can be deployed flexibly and reliably. At present, the best PRV measurement precision is  $> 50 \text{ cm/s}$  [2, 3], corresponding to an optical frequency sensitivity  $> 1 \text{ MHz}$  in the blue spectral range, substantially limited by the thorium argon (ThAr) emission lamp used as the wavelength calibrator for the astrophysical spectrograph. Such emission lamps suffer from uneven line spacing, blended atomic lines from a diversity of ionic states and long-term spectral drift.

An ideal wavelength calibrator provides a high density of bright, regularly-spaced optical lines optimized for the resolution of an astrophysical spectrograph used for PRV (typical resolving power  $R = \lambda/\Delta\lambda \approx 100000$ ). The calibrator’s spectrum should be broad ( $> 100 \text{ nm}$ ) and stabilized to an atomic clock for long-term stability and accuracy, and the instrument should be robust and suitable for long-term operation in the environment of an astronomical observatory. A promising candidate for such an ideal wavelength calibrator is the astro-comb, which consists of an octave-spanning laser frequency comb integrated with a Fabry-Pérot filtering cavity to create the appropriate line-density for use with an astrophysical spectrograph, and locked to an atomic clock for long-term stability (Fig. 1). In previous work we developed astro-combs operating in the deep red ( $\sim 800 \text{ nm}$ ) [4] and in the blue ( $\sim 410 \text{ nm}$ ) [5]. We deployed and successfully operated these red and blue astro-combs at the Tillinghast Reflector Echelle Spectrograph (TRES) and 1.5 m telescope at the Fred Lawrence Whipple Observatory (FLWO) on Mt. Hopkins in Arizona. Here we present the results of wavelength calibrations of the TRES spectrograph using the red and blue astro-combs, highlighting both spectrograph and calibrator

performance near the photon-shot-noise limit, and realizing calibration precision and stability sufficient to enable PRV measurement sensitivity  $< 1$  m/s.

## 2. Astro-comb and spectrograph hardware and operation

An astro-comb [4–12] consists of a high repetition-rate, octave-spanning femtosecond laser frequency comb [13] (“source-comb”) integrated with a filter cavity to match the laser comb line spacing [14, 15] to the resolution of the astrophysical spectrograph (see schematic shown in Fig. 2). In our work the red source-comb is a mode-locked titanium sapphire (Ti:Sapph) laser with a pulse repetition rate of 1 GHz and a pulse width of  $< 6$  femtoseconds, producing light from 700 nm to 1000 nm in the deep red range of the optical spectrum [16]. The light may be frequency doubled to around 400 nm in the blue, *e.g.*, using a  $\beta$ -barium borate (BBO) crystal, to provide the blue source-comb [5]. The 1 GHz source-comb (see Fig. 1(a)) is stabilized to a rubidium atomic clock via radio-frequency techniques [13] providing reference lines spaced by 1 GHz (0.002 nm around 800 nm) with optical frequencies given by

$$f = f_{ceo} + n \times f_{rep} \quad (1)$$

where  $f_{rep}$  is the repetition rate of the laser,  $f_{ceo}$  is the carrier envelope offset frequency, and  $n$  is an integer numbering the comb spectral lines (comb teeth) [13]. Both  $f_{ceo}$  and  $f_{rep}$  are radio-frequencies which are measured and stabilized to the atomic frequency reference and are thus can achieve fractional stability and accuracy better than  $10^{-11}$  with a commercial atomic clock referenced to the Global Positioning System (GPS). The central wavelength portion of the red or blue source-comb light is spatially overlapped with light from a single-mode diode laser, which is offset-locked to the source-comb at a frequency to optimize the Fabry-Pérot cavity (FPC) for maximum astro-comb bandwidth. The diode laser and source-comb are configured to provide light with orthogonal linear polarizations. The overlapping light is sent to a single-mode, polarization maintaining (PM) optical fiber to provide a clean spatial mode. After the fiber, the light is passed through a plane-mirror FPC (Fig. 1(b)) to create a high repetition-rate astro-comb spectrum with adjustable frequency spacing up to 50 GHz. After the filter cavity, the transmitted astro-comb lines have frequencies,  $f_{AC}$ , given by

$$f_{AC} = f_{ceo} + (l + Kn')f_{rep} \quad (2)$$

where  $K$  is the integer line spacing multiplier determined by the ratio of the FPC’s free spectral range (FSR) to the source-comb line spacing ( $f_{rep}$ );  $l$  is the offset of the astro-comb lines in the source-comb; and  $n'$  numbers the astro-comb teeth. Note that Eq. (2) gives the exact frequencies of the main astro-comb lines, without accounting for residual effects from source comb lines suppressed by the FPC (“side modes”). As these side modes are not resolved by the spectrograph, they can systematically shift the line centers recovered by the spectrograph if they are not sufficiently suppressed. An electro-optic modulator (EOM) modulates the frequency of the single-mode diode laser and allows the FPC to be locked to the diode laser with a Pound-Drever-Hall [17] style technique in transmission by adjusting the cavity length via a piezo electric transducer (PZT). Most of the light from the reference laser is separated from the comb light using a polarizing beam splitter after the FPC for stabilization of the cavity, while the astro-comb light is propagated by a multi-mode optical fiber to the calibration system of the astrophysical spectrograph.

The FPC consists of two modified Bragg-stack mirrors on flat substrates spaced to achieve the desired astro-comb line spacing. The FSR is set higher in the blue than the red as the astrophysical spectrograph has constant resolving power  $R = \lambda/\delta\lambda$  corresponding to reduced frequency resolution at higher optical frequencies (shorter wavelengths). In both the red and

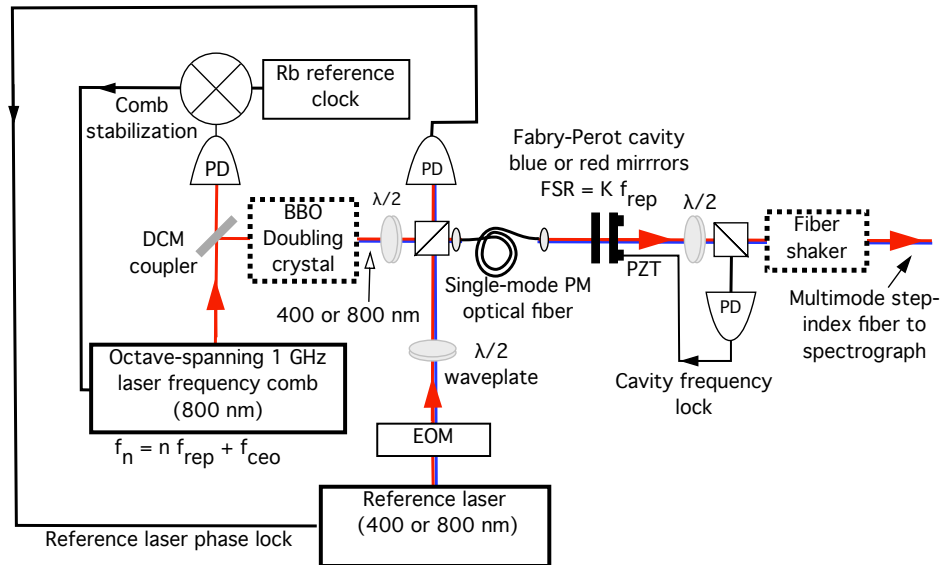


Fig. 2. Block diagram for the red and blue astro-combs operating at around 800 nm and 400 nm, respectively. A 1-GHz repetition-rate Ti:Sapphire laser frequency comb (source comb), with a spectrum centered at 800 nm and stabilized to a rubidium atomic clock, provides emission lines regularly spaced by 0.002 nm. Light from the source-comb, either directly or after frequency doubling in a BBO crystal to 400 nm to provide the blue source-comb, is spatially overlapped with light from a single wavelength reference diode laser and sent via a single-mode optical fiber through a Fabry-Pérot cavity to create an astro-comb spectrum with an adjustable effective repetition rate up to 50 GHz (*i.e.*, spectral line spacing up to 0.1 nm). A multi-mode fiber, which can be physically shaken to produce optical mode scrambling, sends the astro-comb light to the wavelength calibration system of the TRES spectrograph.

blue astro-combs the FSR is set to roughly three times the spectrograph resolution, slightly larger than the optimal spacing for maximum calibration sensitivity [6] so that the wings of each astro-comb line on the spectrograph may be clearly resolved to more carefully study the astro-comb line profile. For the red astro-comb, the mirrors are spaced by approximately 5 mm to achieve an FSR of 30 GHz. The blue astro-comb FPC mirrors are spaced by 3 mm to provide an FSR of 50 GHz. The FPC finesse is approximately 250 corresponding to a linewidth of 150 MHz, which yields about 22 dB suppression of the nearest source comb lines not resonant with the FPC. Imbalance in side mode suppression can lead to systematic shifts in the centroids of the astro-comb lines as recovered on the spectrograph, and thus must be carefully characterized as described below.

To enable filtering of large ( $\approx 100$  nm) optical bandwidths, the FPC mirrors are formed on flat substrates. Ideal flat mirrors lead to degenerate transverse modes, with all resonant longitudinal modes spaced by  $c/2\lambda$ . However, a flat mirror FPC must be aligned to approximately  $1 \mu\text{rad}$  so that the finesse is not limited by variations in cavity length across the transverse beam profile. Curved mirrors can reduce alignment requirements, but the comb light must then be focused optimally into the cavity to avoid other transverse cavity modes. This is challenging across a broad 100 nm spectrum as the focal waist coupled out of the fiber and the waist of the lowest transverse modes have different scalings with wavelength. Across large bandwidths, flat



mirror cavities significantly reduce complexity in cavity coupling.

We used the astro-comb to calibrate the TRES spectrograph, a fiber-fed, cross-dispersed, echelle spectrograph with wavelength coverage from 390 nm to 900 nm located at the 1.5 m Tillinghast telescope at the Whipple Observatory [18]. TRES consists of a low rule-density diffraction grating blazed for use in high order to provide high dispersion and thus high resolution with FSR in each diffractive order  $\approx 10$  nm. A cross-dispersing prism separates the orders of the grating, creating a two-dimensional spectrum matched to the geometry of a CCD used to record spectra. A 100  $\mu\text{m}$  multi-mode optical fiber feeds light from the telescope to the spectrograph. The size of the fiber image on the CCD (Fig. 3(a)) leads to a resolving power  $R = \lambda/(\Delta\lambda) \approx 45000$ , producing a resolution of 9 GHz at 800 nm and 18 GHz at 400 nm. The TRES environmental enclosure provides a stable operating temperature  $\approx 0.01$  C over an observing night. The enclosure is not pressure stabilized, however, leading to uncontrolled variation in the spectrograph calibration at the 100 m/s ( $\sim 100$  MHz or  $2 \times 10^{-4}$  nm at 800 nm) level over the course of a few hours. Additionally, relaxation of the spectrograph's mechanical structure and cryogen fills of the CCD dewar lead to additional drifts of the wavelength calibration of roughly 100 m/s during a typical observing night. Thus, sub-m/s PRV sensitivity requires approximately a factor of 1000 correction for instrumental drift over an observing night.

For the red astro-comb, the spatial structure of the calibration light was scrambled by an integrating sphere before injection into the spectrograph optical fiber feed, which reduced the optical throughput by  $> 10^4$  and therefore required several minute integration times to achieve sufficient signal on the CCD for high-precision wavelength calibration. Prior to blue astro-comb calibrations at the TRES spectrograph, the integrating sphere was removed during a spectrograph upgrade, increasing the optical throughput while preserving stable, uniform, illumination of the spectrograph fiber by calibration light. A mechanical fiber-shaker was installed to provide dynamic scrambling of transverse optical modes in the optical fiber [19] coupling astro-comb light to the spectrograph. The results presented here for the blue astro-comb use the shaker while red astro-comb data were taken with the integrating sphere and without the shaker.

### 3. Astro-comb wavelength calibration of spectrograph

During two sessions at the Whipple Observatory in 2009 and 2010 we accumulated several weeks of astro-comb calibration spectra using the TRES spectrograph. These spectra were primarily acquired during the day or while the telescope dome was closed due to poor weather conditions, though some calibration spectra were acquired during observing hours.

We used standard techniques to acquire two-dimensional (2-D) astro-comb images on the TRES CCD and reduce the data into one dimensional (1-D) spectra [20]. At the beginning of each calibration sequence, we took ten "biases," zero-time exposures with the shutter closed, to determine the zero value of each CCD pixel. Next, we acquired ten "flats," exposures of the spectrograph to a continuum halogen lamp over several minutes. Offline, we summed the flats after subtracting biases and rejecting outliers (*e.g.*, cosmic rays) to generate a high signal-to-noise measure of the response of the spectrograph to white light. The flats served two purposes: identifying positions of the echelle orders on the CCD and pixel normalization. Lastly, we acquired a 2-D astro-comb image, which required 300 seconds when using the red astro-comb due to the presence of the integrating sphere and 10 seconds when using the blue astro-comb. We typically repeated this calibration procedure many times during a several-hour calibration session. We modeled positions on the CCD of each echelle order as a product of polynomials in both the dispersion and cross-dispersion directions fitted from the 2-D spectral images of the flats. These polynomials were used to sum pixels in the cross-dispersion direction to produce 1-D spectra for each echelle order. We summed both flats and astro-comb spectra (after sub-

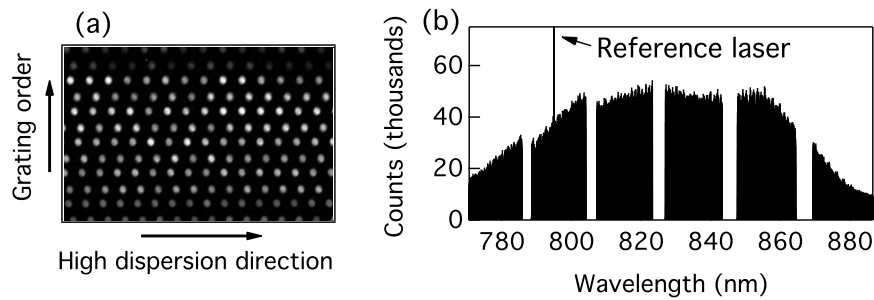


Fig. 3. Example spectrum for the red astro-comb, acquired with the TRES spectrograph. (a) Small region of the 2-D spectral image encompassing 300 by 200 pixels on the CCD corresponding to the central 1 nm of each of the six spectrograph grating orders containing significant astro-comb intensity. Each astro-comb tooth (spectral peak) has a point spread function (PSF) corresponding to the image of the optical fiber convolved with the optical response of the spectrograph optics. (b) Red astro-comb spectrum covering six spectrograph orders and reduced to 1-D. FWHM of spectrum is approximately 100 nm with about 50 000 peak counts acquired in a 300 s exposure. Gaps in spectrum are regions in which calibration light is not focused onto the CCD [18]. The strong line at 795 nm is the reference laser used to stabilize the Fabry-Pérot filter cavity and provide a fiducial marker of known absolute wavelength.

tracting biases and rejecting outliers) to produce 1-D spectra. We then divided 1-D astro-comb spectra by normalized 1-D flats, point by point, to account for gain variations in the CCD as well as effects of optical fringing in the CCD (see Sec. 3.2), which is crucial in the red where the absorption of the CCD is relatively low.

Figure 3 shows an example of a red astro-comb 2-D image observed with the TRES spectrograph, and the resulting 1-D spectrum composed of roughly 1200 spectral peaks (i.e., calibration lines), which are evenly spaced in frequency by 32 GHz (0.07 nm at 800 nm) and cover six echelle orders of the spectrograph. Each spectral peak has a full width of approximately 10 GHz (6 CCD pixels) determined primarily by the fiber image on the CCD, with a peak of > 40 000 counts per point in a 1-D spectrum after a 300 s exposure in the central wavelength region of the comb.

The expected frequency uncertainty,  $\delta\nu$ , from photon shot-noise, in determining the centroid of a single astro-comb 1-D spectral peak [6, 21] is

$$\delta\nu = A \frac{\text{FWHM}}{S/N \times \sqrt{n}} \quad (3)$$

where  $A$  is a normalization constant of order unity, FWHM is the peak width, S/N is the peak signal-to-noise ratio, and  $n$  is the number of 1-D points sampling the peak. For the TRES spectrograph with an instrument profile dominated by the fiber profile, we find from simulations that  $A \approx 0.4$ . The resulting sensitivity from a photon-shot-noise limited measurement for one red astro-comb peak of width 10 GHz, spanning 6 pixels, and with 50 000 counts is then 7 MHz (PRV sensitivity  $\approx 7$  m/s). In the ideal case of no systematic effects, the shot-noise-limited precision of a wavelength calibration improves as  $N^{1/2}$ , where  $N$  is the number of astro-comb spectral peaks leading to 50 cm/s PRV sensitivity for 200 peaks spanning one full echelle order in the center of the astro-comb spectrum and below 30 cm/s when all six orders of the red astro-comb are combined.



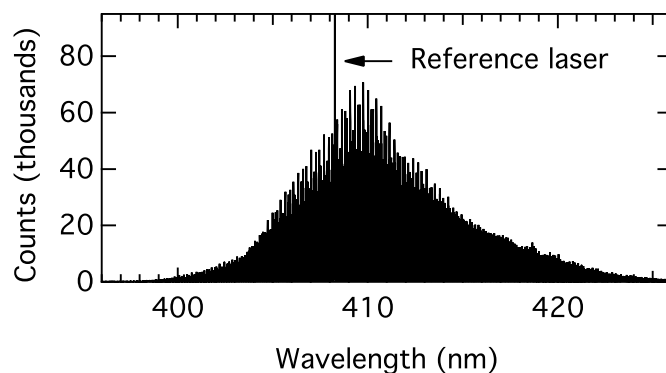


Fig. 4. Example 1-D spectrum of the blue astro-comb, acquired with the TRES spectrograph. FWHM of the spectrum is approximately 10 nm with 40000 to 60000 peak counts acquired in a 10 s exposure with the astro-comb light attenuated by a factor of 10.

Figure 4 shows an example blue astro-comb 1-D spectrum acquired using the TRES spectrograph, covering about 10 nm and centered around 410 nm. With the greater optical throughput from the blue astro-comb to the spectrograph (because the integrating sphere was removed), each 1-D spectral peak reaches a maximum of 40000 – 60000 counts per 1-D point in a 10 s exposure, leading to a 16 MHz (PRV sensitivity  $\approx 6$  m/s at 410 nm) sensitivity for one blue astro-comb peak of width 20 GHz and spanning 6 pixels. With roughly 600 astro-comb lines in the calibration spectrum (Fig. 4), the expected photon-shot-noise limit for the wavelength calibration sets a PRV sensitivity of 50 cm/s in a single calibration exposure.

### 3.1. Fitting astro-comb spectra

To calibrate the wavelength scale of the spectrograph we fit a measured astro-comb 1-D spectrum to extract a “frequency solution”: an assignment of frequency (and thus wavelength in vacuum) to each CCD pixel. Each astro-comb spectral peak (*i.e.*, calibration line) is separated from its neighbor by a constant frequency determined by Eq. (2) with at least 10 digit accuracy, as both the repetition rate and offset frequency are locked to a rubidium atomic clock. Therefore, the centroids of astro-comb lines are spaced evenly in the frequency domain. A smoothly varying polynomial then provides a reliable frequency solution accounting for dispersion in the spectrograph. To perform the frequency solution fit, we first reduce astro-comb 2-D image data to a 1-D spectrum. The 2-D point spread function (PSF) of the TRES spectrograph is the convolution of the profile of light exiting the fiber, which is re-imaged onto the CCD, with the optical response of the spectrograph binned into CCD pixels. Importantly, astro-comb calibration lines are spectrally much narrower than the resolution of the spectrograph - effectively frequency delta functions - allowing the spectrograph line profile to be determined directly. We model the 1-D reduced instrument profile of each astro-comb line as the convolution of a distorted half circle representing the output of the optical fiber bringing astro-comb light into the spectrograph integrated in the cross-dispersion direction, with a sum of Hermite-Gaussian modes to represent contributions from the spectrograph optics (Fig. 5). This convolved profile is then integrated across each 1-D point for fitting to the 1-D astro-comb spectrum. All the parameters describing the instrument profile for an individual astro-comb line are re-parameterized as smoothly varying polynomials across each order of the spectrograph, with the amplitudes of each line allowed to vary independently. Resulting fit parameters for both red and blue astro-

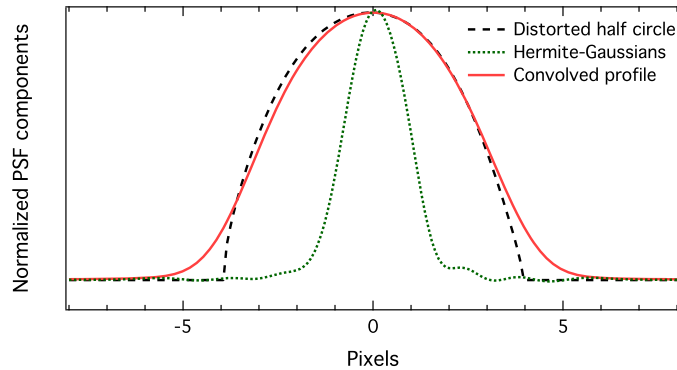


Fig. 5. Example model fit (red solid line) of TRES spectrograph 1-D reduced instrument profile. Model consists of the convolution of a distorted half circle representing the 1-D reduced optical fiber profile (black dashed line) and a sum of Hermite-Gaussians representing the optical response of the TRES spectrograph (green dotted line). The convolved line profile is then numerically integrated to determine the value at each point in a 1-D spectrum.

comb data confirm expectations based on the spectrograph's physical properties: we find that the spectrograph instrument profile is dominated by the half-circle component representing the 100 micron optical fiber and a 15 micron width from the Hermite-Gaussian modes representing the spectrograph optics. Our fits yield slow variation with wavelength in the astro-comb spectral peak width from both the half-circle and Hermite-Gaussian components of roughly 20%. These results are consistent with models of the spectrograph focus, anamorphism, and variable dispersion showing roughly 1 pixel variation across an echelle order, with the spot size becoming larger at shorter wavelength on the blue end of the spectrograph [18].

A key requirement for achieving photon-shot-noise limited spectrograph calibration is scrambling of the coherence of the input astro-comb light to prevent unwanted optical interference patterns on the spectrograph CCD, which leads to added intensity noise in the measured astro-comb spectrum. Individual transverse modes of the optical fiber, used to transport the astro-comb light to the spectrograph, have differing path lengths, leading to non-trivial optical interference patterns on the focal plane of the CCD [19] if the input astro-comb light is coherent (Fig. 6(a)). In blue astro-comb operation, we mechanically shake at 15 Hz the multi-mode optical fiber coupling light from the astro-comb to the spectrograph. This shaking causes the propagating modes of the optical fiber to have time-varying path lengths, which greatly reduces the time-averaged interference of coherent calibration light, producing a relatively flat intensity output from the fiber over a 10 s calibration exposure (Fig. 6(a)). To study the noise properties of the blue astro-comb as measured by the spectrograph with the mechanical shaking of the fiber turned off and on, we normalized the heights of all astro-comb 1-D spectral lines provided by the data fit procedure described above. We then folded all normalized astro-comb lines on top of each other with their peak centers aligned and widths normalized so as to create a single peak (Fig. 6(b)). Comparing such normalized and folded astro-comb spectra with fiber shaking off and on, we find that shaking improves the calibration signal-to-noise ratio by a factor of 3-5. Using the fit model described above with blue astro-comb spectra acquired with active mode scrambling, we realized near photon-shot-noise limits on the fit to one echelle order from the TRES spectrograph (Fig. 7), with residuals within 10% of photon-shot-noise near the folded line center and growing somewhat in the wings, as determined point-by-point directly from the

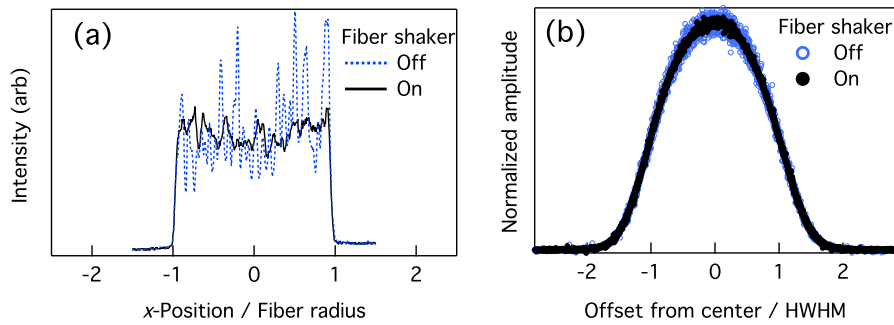


Fig. 6. (a) Cross-section of the image of a  $100\ \mu\text{m}$  multi-mode optical fiber with mechanical shaker off and on, showing reduced intensity variation across the fiber surface in the presence of shaking, observed with a laboratory CMOS camera. (b) Reduced noise in the blue astro-comb spectrum on the TRES spectrograph with mechanical shaking. Astro-comb lines are normalized and folded on top of each other, as described in the main text. Residuals of data from fit model are approximately 5 times expected photon shot-noise in the absence of shaking and within 10% of photon shot-noise with the shaker on.

measured line profile with a noise model including photon-shot-noise as well as read noise and in good agreement with Eq. (3).

### 3.2. Optical fringing of red light in CCD

At red wavelengths ( $> 700\ \text{nm}$ ) the TRES spectrograph suffers significantly from “fringing:” thin-film optical interference inside the CCD leading to strong, rapid changes with wavelength in the CCD efficiency. As the wavelength scale of the spectrograph drifts due to environmental changes (pressure, temperature, etc.), the location of these fringes on the CCD varies slightly, corrupting the wavelength calibration. Normalization of astro-comb spectra with flat-field (white light) images acquired with a halogen bulb reduces the systematic error due to these variations, but the effect of fringing remains a critical limit on performance of the spectrograph in the red. Additionally, light scattered in the spectrograph (*e.g.*, off of imperfections in the grating) together with fringing in the CCD reduces the signal to noise in red astro-comb spectra compared to the nominal photon shot-noise. Scattered light in the spectrograph reaches the CCD from outside the spectral band expected from the calibration, resulting in variable, wavelength-dependent contrast that is different than that from the guided light and hence is not optimally corrected by flat fielding. This performance limit of the TRES spectrograph, which uses an EEV 42-90 CCD, could be reduced with a deep depletion CCD at the expense of reduced response in the blue spectral range. (*Mention of commercial products or services in this paper does not imply approval or endorsement by NIST, nor does it imply that such products or services are necessarily the best available for the purpose.*)

### 3.3. Spectrograph stability

To characterize the stability of the TRES spectrograph, we performed repeated wavelength calibrations using the red astro-comb over a week. We injected light into two channels of the spectrograph: the “science” fiber, which when not being calibrated is guided on a target star; and a “sky” fiber used to measure background light (*e.g.*, moonlight or bright, nearby stars). We evaluated overall changes in the frequency solution of the spectrograph by calculating the

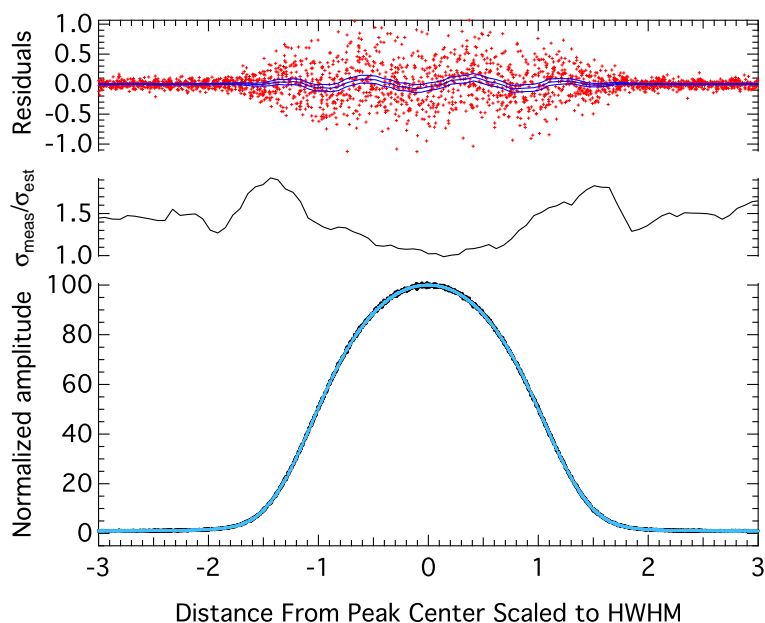


Fig. 7. Fit to one order of the blue astro-comb spectrum, using the model and procedure described in the main text. Bottom panel: folded spectrum in which the centroids of all 200 astro-comb lines are aligned, and their amplitudes and widths normalized. Top panel: folded fit residuals (points) and mean and 95% confidence levels (solid lines). Middle panel: averaged residuals normalized to the expected photon shot-noise, showing near shot-noise performance near the folded line center.

central frequency of each spectrograph order and determining the average change of all calibrated orders. The results of a week of such calibrations are summarized in Fig. 8(a), showing changes in the frequency solution of several hundred m/s, corresponding to several hundred MHz changes in the mean optical frequency, both over the course of a night and over the full week. These results are consistent with expectations of the TRES spectrograph's performance as observed with ThAr wavelength calibrations [18]. Error estimates in PRV precision derived both from Monte Carlo for the frequency solution of each order and the standard deviation of changes of each order from the mean  $\approx 1$  m/s for the red astro-comb frequency solution for the full six spectrograph orders (corresponding to roughly 1 millipixel on the CCD). This error is approximately a factor of 2 above expectations from photon shot-noise (see Eq. (3)), limited by excess noise caused by (i) spatial variations in the intensity profile of astro-comb light leaving the fiber (as the shaker was not used with the red astro-comb), and (ii) fringing at the red end of the CCD, as described above. Nevertheless, our fit model successfully recovered red astro-comb spectra in the presence of this excess noise at the 1 m/s level. Despite the 1 m/s sensitivity of the red astro-comb frequency solutions, the solutions for the science and sky channel wavelength solutions diverge by 6 m/s over the course of one night (Fig. 8(b)). This is likely caused by the off-axis positioning of the sky channel [18], which is therefore not illuminated uniformly by the calibration light. Significant re-engineering of the calibration unit at the TRES spectrograph has recently been implemented which should reduce such drifts.

Using the blue astro-comb we demonstrated near photon-shot-noise limited wavelength calibration of the TRES spectrograph. At the shorter blue wavelengths the silicon of the CCD is

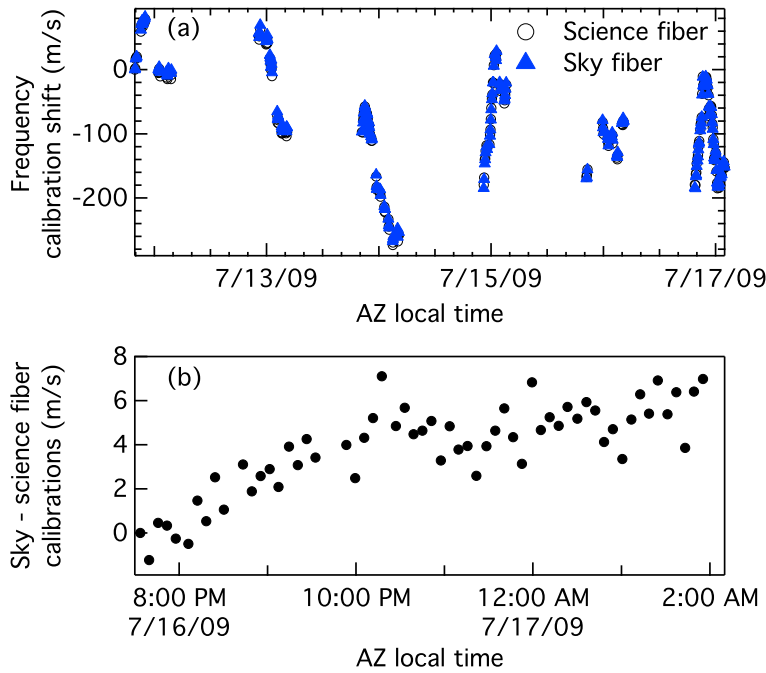


Fig. 8. (a) Measured drift over five nights of the TRES spectrograph frequency solution from red astro-comb calibrations in the 800-900 nm spectral range, expressed as an effective PRV shift. Calibrations are shown using two input optical channels to the spectrograph: the science and sky fibers. (b) Drift between frequency solutions for science and sky fibers over one night, likely due to input coupling of off-axis sky channel. Comparable drifts were seen across all five nights, with the divergence between the two fibers never  $> 10$  m/s. Uncertainties in the data points of (a) and (b)  $\approx 1$  m/s.

strongly absorbing, which greatly suppresses fringing. Additionally, we implemented the mechanical shaker described above to eliminate interference between modes in the optical fiber coupling light from the blue astro-comb to the spectrograph. We repeatedly calibrated the spectrograph over several consecutive nights using the blue astro-comb: *e.g.*, Fig. 9(a) shows a sample of the measured drift in the spectrograph wavelength calibration over a period of about one hour, consistent with the spectrograph's sensitivity to changes in the ambient environment. Because of improved coupling of the blue astro-comb light to the spectrograph compared to the earlier red astro-comb measurements, much larger optical throughput was achieved in the blue astro-comb measurements, and hence much faster spectrograph calibrations, such as the 10 s exposures reported here. Note, however, that readout of the spectrograph CCD took close to one minute, limiting the calibration speed. Typical measured spectrograph drift during the readout period was near 1 m/s. Residuals in the frequency solutions provided by the blue astro-comb were  $\approx 1$  m/s in each spectrograph order (Fig. 9(b)), and within 10% of that expected from photon shot-noise as verified with Monte Carlo simulations of the astro-comb spectrum using a noise model including photon-shot-noise and read noise. This enables 50 cm/s calibration of the TRES spectrograph using the full spectrum of the blue astro-comb across four spectrograph orders.

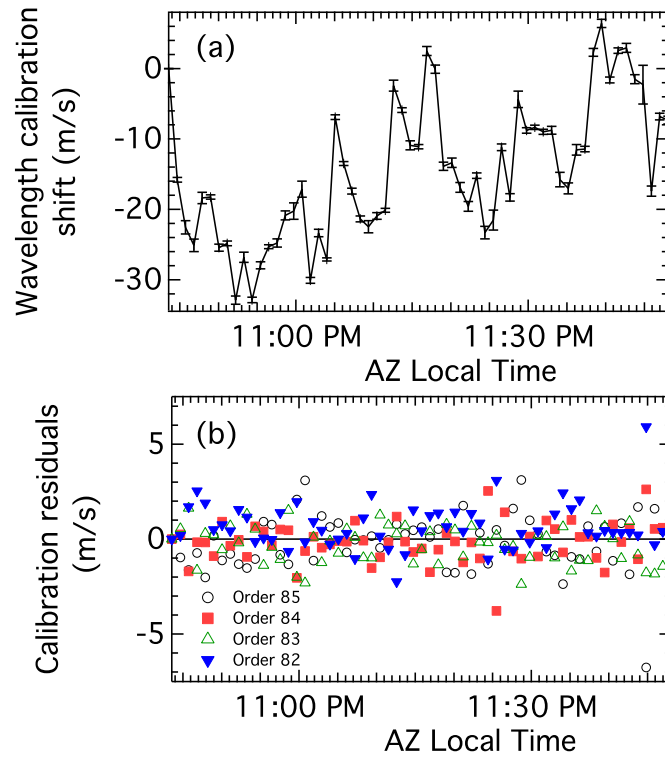


Fig. 9. Measured drift over about one hour of the TRES spectrograph frequency solution from blue astro-comb calibration. (a) Frequency solution (expressed as an effective PRV shift) from averaging four spectrograph orders of blue astro-comb data between 400 and 420 nm. Error bars indicate the standard deviation of the averaged orders. Observed PRV variations  $\sim 30$  m/s over spans of several minutes are consistent with known drift rates of the TRES spectrograph [18]. (b) For each spectrograph order, variations of frequency solutions from the average solution (expressed as effective PRV shifts)  $\approx 1$  m/s.



### 3.4. Accuracy of calibrations

Realizing long-term stability of spectrograph calibrations using an astro-comb requires an assessment of the underlying accuracy of the astro-comb itself, and the time variation of any inaccuracies. Source comb line positions are determined by radio-frequencies stabilized to an atomic clock, and as such have more than sufficient accuracy for 5 cm/s searches for exo-Earths. However, neighboring source comb lines are not resolved on high-resolution echelle spectrographs, and thus residual transmission in the tail of a filter cavity resonance can skew the measured centroid of an astro-comb line. In particular, the spacing between FPC resonances, the FSR, unavoidably varies across the full astro-comb spectrum due to wavelength dependence in the penetration depth of light into the mirror coatings. This wavelength dependence of the FSR can induce systematic errors in the spectrograph calibration because the FPC resonance is not centered on all astro-comb resonances across its full spectrum, causing source comb side modes nearest to some astro-comb peaks to be suppressed by differing amounts (*i.e.*, side mode asymmetry) [7, 9].

We recently demonstrated an *in-situ* technique to determine the systematic shifts of astro-comb lines due to such FPC dispersion, which can be applied at a telescope-based spectrograph to enable wavelength calibration accuracy better than 10 cm/s [22]. By measuring the intensity of astro-comb lines as the FPC length is adjusted, we determine: (i) the offset of each FPC resonance from the nearest source comb line; (ii) FPC finesse as a function of wavelength; and (iii) the intensity of individual source comb lines. These parameters can be determined quickly and reliably over the full bandwidth of the astro-comb with only  $\approx 20$  measurements at slightly different FPC lengths, and can be performed quickly and reliably. We performed several such measurements on the blue astro-comb and found that corrections  $\approx 1$  m/s were required to the nominal astro-comb frequencies to compensate for these systematic shifts [5].

### 3.5. Absolute spectrograph calibration

To provide an absolute calibration of the TRES spectrograph, an individual astro-comb frequency must be determined. From knowledge of a single astro-comb line the rest may be ascertained with atomic clock precision via the comb relation (Eq. (2)):

$$f_{AC} = f_{ceo} + (l + Kn')f_{rep}.$$

The offset and spacing frequencies,  $f_{ceo}$  and  $f_{rep}$  are measured via radio-frequency techniques described above with at least cm/s accuracy. The integers  $K$  and  $l$  representing the number of source comb lines filtered by the cavity and the offset of the cavity from zero frequency must be determined, along with identifying the line number,  $n'$  associated with one astro-comb peak on the spectrograph. The remaining peaks are then counted using the spectrograph measurements and Eq. (2) applied to determine their frequencies. To determine  $K$ ,  $l$ , and  $n'$  for the blue astro-comb, we began with a coarse frequency solution derived from a ThAr lamp [23], which we used to determine the frequency of the reference diode laser with sufficient accuracy to determine the nearest blue source comb line ( $< 500$  MHz or 200 m/s accuracy). Note that a commercial wavemeter may also be used to determine the diode laser wavelength (and hence frequency) with this accuracy. Applying the ThAr wavelength solution, we found a nominal diode laser frequency (wavelength in vacuum) of 734 199.8(2) GHz (408.3254(1) nm).

Applying Eq. (2) and recognizing that the offset frequency  $f_{ceo}$  is doubled in the conversion from red to blue light, we found  $K = 49$ ,  $l = 20$ , and  $n' = 14314$ , thus determining the nearest source comb line to the reference diode laser. The frequency of this source comb line was thereby determined absolutely with reference only to the laser frequency comb parameters (all tied to the atomic clock) and independently of the ThAr calibration, leading to an absolute frequency of the comb line nearest the reference diode laser spectral line of 734 199.775(1) GHz

limited by the absolute accuracy of the Rb frequency reference used for these measurements. This result is in good agreement with the Th:Ar calibration. The absolute frequencies of all other calibration lines from the blue astro-comb were then determined simply by counting comb teeth. Absolute frequency errors associated with finite side mode suppression described above as well as source-comb line-to-line intensity variation and etaloning in the FPC substrates [22] were also  $< 0.001$  GHz for all spectral features used, thus providing an absolute calibration of the TRES spectrograph across the full calibration spectrum. Stabilizing the Rb frequency reference to the Global Positioning System (GPS) and straightforward improvements in FPC implementation will improve astro-comb accuracy by more than an order of magnitude.

Comparisons of astro-comb calibrations to those from Th:Ar lamps and characterizations of astro-comb systematic errors demonstrate an accuracy and reproducibility of calibrations with the astro-comb below the 1 m/s level. To determine the radial velocity of an astronomical target star, the high accuracy astro-comb calibrations must be applied to the stellar spectrum. This requires, in addition to a very stable, high-performance astrophysical spectrograph, that calibration light and stellar light exit the optical fiber coupling the telescope to the spectrograph with the same transverse mode profile. Key to this behavior is mode scrambling in the optical fibers. State of the art fiber-fed astrophysical spectrographs often rely on double image scramblers [24] to ensure that transverse modes of the optical fibers are consistently filled. With such techniques, long-term performance is presently at the 1 m/s level [1] due to a combination of Th:Ar calibrator performance, telescope guiding, and mode scrambling. To further improve fiber mode scrambling, multi-mode optical fibers with square and octagonal cross-sections are being studied. The authors plan to investigate the long-term stability of calibrations by comparing stable radial velocity stars to an astro-comb at such a spectrograph.

#### 4. Conclusions

We used two astro-combs, each consisting of a laser frequency comb integrated with a Fabry-Pérot filtering cavity, to calibrate the absolute frequency (or wavelength) of a high-resolution astrophysical spectrograph over a 100 nm band in the deep red and over 20 nm in the blue. We reliably operated the astro-combs over several weeks in 2009 and 2010 at the Fred Lawrence Whipple Observatory (FLWO) on Mt. Hopkins in Arizona, and repeatedly calibrated the TRES spectrograph. Expressed in terms of measurement sensitivity to changes in the precision radial velocity (PRV) of stellar sources, relevant to searches for small exoplanets, the astro-combs provided spectrograph calibration sensitivity  $< 1$  m/s, limited primarily by the environmental sensitivity of the TRES spectrograph, and obtaining absolute agreement with thorium argon lamp calibration.

In ongoing work, we are preparing both to calibrate broader, visible wavelength bands and to apply the obtained sub-m/s calibration sensitivity to stellar PRV observations. To this end we have assembled and are presently characterizing a “green astro-comb” comprising a 1 GHz repetition rate Ti:Sapphire laser, a coherent wavelength shifting element based on a short, tapered photonic-crystal fiber (PCF) [25], and a broadband Fabry-Pérot filter cavity based on zero dispersion group delay mirror sets [26, 27]. Improved spectrograph wavelength calibration is not limited to exoplanet research — a broad cross section of astrophysical problems may be addressed, perhaps including the nature and dynamics of dark energy [28, 29], and the constancy of fundamental constants over cosmological time scales.

#### Acknowledgments

This work was performed with support from NSF grants AST-0804441, ATI-0905214 and ATI-1006503; NASA grant NNX09AC92G; and internal support from the Smithsonian Astrophysical Observatory. GF acknowledges financial support from the Hungarian OTKA-NFU Mobility

grant MB08C 81013. We would like to thank Keith Lykke for the use of a wavemeter during this project.